JOURNAL OF PHYSICAL ORGANIC CHEMISTRY, VOL. 4, 293–300 (1991)

KINETIC MODELLING OF THE LOW-TEMPERATURE PHOTO-OXIDATION OF HEXAFLUOROPROPENE

A. FAUCITANO AND A. BUTTAFAVA
DPTM di Chimica Generale, V.le Taramelli 12, 27100 Pavia, Italy
V. COMINCIOLI
DPTM di Matematica, Università di Pavia, Pavia, Italy
AND
G. MARCHIONNI AND R. J. DE PASQUALE
Montefluos, CRS, Bollate (Milan), Italy

By kinetic simulation, the significant features of the mechanism of the low-temperature photo-oxidation of hexafluoropropene were elucidated and the rate constants for the major elementary reactions of the intermediate fluorinated peroxy and alkoxy radicals were determined through a best-fit procedure. Comparison with analogue reactions in non-fluorinated systems showed a significant increase in reactivity for the self-reaction and double bond addition by peroxy radicals and β-scission by alkoxy radicals, which are discussed in terms of fluorine substituent effects.

INTRODUCTION

The photo-oxidation of perfluoropropene is a complex free-radical process leading to oligomeric peroxidic perfluoropolyethers and —COF-containing isolable products:[1]

$$CF_2CF(CF_3) + O_2 \xrightarrow{h\nu} CF_3O(CF_2CF(CF_3)O)_l(CF_2O)_m(O)_nX + CF_2O + CF_3COF$$
$$X = -COF,\ -CF_2COF$$

Previous work on this reaction[1–6] succeeded in identifying some of the basic features of the mechanism. However, because of its complexity, the full reaction scheme is far from being completely clarified. Further, no derivation of rate constants has yet been attempted. The aim of this work was to extend the understanding of the mechanism and to obtain rate constants for the fundamental steps. The method used was the kinetic simulation of the experimental process by applying a best-fit procedure based on numerical integration of the system of differential equations without a steady-state approximation. The results of this investigation are considered of interest for the rationalization of the free-radical chemistry in perfluoroalkene–oxygen systems and for the understanding of the effects of fluorine substitutions on the reactivity of oxygen- and carbon-centred radicals.

EXPERIMENTAL

The photo-oxidation of neat perfluoropropene was carried out at −40 °C in the liquid state in an oxygen atmosphere using a high-pressure mercury lamp.[1a] During the reaction the oxygen flow was continuously monitored in order to determine the oxygen uptake. Samples of the reaction mixture were extracted periodically from the reaction vessel for the analysis of the reaction products, which included gravimetric determination of the oligomer formed and the monomer reacted, ^{19}F NMR analysis of the structure of the oligomers after extraction of the unreacted monomer, with quantitative determination of the ether bond yield,[1a,b] and determination of the total peroxide content by iodometry in $CF_2ClCFCl_2$–acetic anhydride (1 : 2) solvent. The total yield of —COF carbonyl products was determined by titration with an excess of standard KOH solution followed by titration of the F^- ions with $Th(NO_3)_4 \cdot 4H_2O$ using sodium alizarinsulphonate as indicator; most of the —COF products (>80 per cent) were identified as COF_2 by gas chromatography (Kel-F/3 oil on Chromosorb W, 20 °C). At the end of the reaction the weight-average molecular weight, M_w, of the oligomers was determined by NMR spectroscopy.

In agreement with previous reports,[1a,b] the NMR

0894–3230/91/050293–08$05.00

Received 21 June 1990
Revised 3 December 1990

spectra of the oligomers are consistent with polyether structures having as major repeating units $-[CF_2CF(CF_3)O]-$. Minor amounts (< 5 per cent) of $-[CF_2O]-$ units are also present.

The peroxides account for 10–30 per cent of the overall oxygen absorbed and their structures are consistent mainly with the formulae $-OCF_2CF(CF_3)OO-$ and $-OCF_2OO-$.

Eight runs were performed under different experimental conditions by adopting variable UV light intensity ($0{\cdot}29 \times 10^{-4}$ E* s^{-1} and $0{\cdot}76 \times 10^{-5}$ E s^{-1}) and variable optical path lengths (1–4 cm) and reaction volumes. Part of the experimental results are shown in Figure 1 and also in Tables 2 and 3 together with the computed results. For conciseness, in Table 3 only the data regarding the end reaction times are reported.

REACTION SCHEME AND KINETIC MODEL

The mechanism used as a basis for the kinetic model is shown in Table 1. In agreement with previous proposals,[1] the major reaction path for the formation of peroxides is assumed to be the addition of peroxy radicals to perfluoropropene according to

$$R_f^{\cdot} + O_2 \longrightarrow R_fO_2^{\cdot} \underset{O_2}{\overset{M}{\longrightarrow}} R_fOOM^{\cdot}$$

Other minor contributions to the peroxide yield are derived from radical couplings. The chain mechanism for the generation of ether bonds is based on the non-terminative disproportionation of peroxy radicals followed by addition of alkoxy radicals to PFP:

$$R_fO_2^{\cdot} + R_fO_2^{\cdot} \longrightarrow 2R_fO^{\cdot} \underset{O_2}{\overset{M}{\longrightarrow}} ROM^{\cdot}$$

Within this proposed scheme, the process is started by the reaction of hexafluoropropene (HFP) with O_2 but with increasing reaction time the peroxidic products rapidly become the dominant photoactive compounds in the system. The formation of COF_2, CF_3CFO and the terminal acid fluorides and fluoroformates are accounted for by the β-scission of alkoxy radicals [reactions (6) and (7)]. No distinction was made in the model between *head* and *tail* additions of peroxy radicals and alkoxy radicals to the monomer since cumulative yields of peroxides, $-COF$ and ethers were used as reference data. Consequently, no distinction is made between the different types of β-scissions [reactions (6) and (7)]. According to recent NMR analysis, the head additions predominate by a factor of about 7,[6–8] and additionally reaction (7) is faster than reaction (6) (see below). Termination is assumed to be based essentially on bimolecular radical couplings: all types of direct and cross coupling among peroxy, alkoxy and alkyl radicals were considered [reactions (9)–(13)].

The rate constants for terminal couplings without disproportionation [reactions (10)–(13)], were assigned a fixed value of 10^7 l mol^{-1} s^{-1} which is in the range expected for diffusion-controlled couplings of macroradicals in solutions.[9] The oxygen addition to radicals [reactions (3)] was also assigned a fixed value of 10^8 l mol^{-1} s^{-1} in agreement with literature reports.[10]

*E = einstein

Table 1. Reaction scheme and best-fit rate constants derived from the kinetic model[a]

No.	Reaction[6]			Rate constants (l mol^{-1} s^{-1})
1	$CF_2{=}CF(CF_3)$	$\xrightarrow{O_2}$	$CF_3^{\cdot} + CFO^{\cdot} + CF_2O$	
2	RfOORf	$\longrightarrow$	$2\,RfO^{\cdot}$	
3	$Rf^{\cdot} + O_2$	$\longrightarrow$	$RfO_2^{\cdot}$	10^8
4	$RfO_2^{\cdot} + M$	$\longrightarrow$	$RfOOCF_2\dot{C}F(CF_3)$ $RfOOCF(CF_3)\dot{C}F_2$	$0{\cdot}3 \pm 0{\cdot}05$
5	$RFO^{\cdot} + M$	$\longrightarrow$	$RfOCF_2\dot{C}F(CF_3)$ $RfOCF(CF_3)\dot{C}F_2$	95 ± 4 (s^{-1})
6	$RfOCF_2CF(CF_3)O^{\cdot}$	$\longrightarrow$	$RfO\dot{C}F_2 + CF_3CFO$ $RfOCF_2CFO + CF_3^{\cdot}$	57 ± 5 (s^{-1})
7	$RfOCF(CF_3)CF_2O^{\cdot}$	$\longrightarrow$	$RfO\dot{C}F(CF_3) + CF_2O$	57 ± 5 (s^{-1})
8	$RfO_2^{\cdot} + RfO_2^{\cdot}$	$\longrightarrow$	$2RfO^{\cdot} + O_2$	$(2{\cdot}8 \pm 0{\cdot}4) \times 10^6$
9	$RfO_2^{\cdot} + RfO_2^{\cdot}$	$\longrightarrow$	$RfOORf + O_2$	$(6{\cdot}7 \pm 1{\cdot}2) \times 10^4$
10	$RfO_2^{\cdot} + Rf^{\cdot}$	$\longrightarrow$	RfOORf	10^7
11	$RfO^{\cdot} + Rf^{\cdot}$	$\longrightarrow$	RfORf	10^7
12	$RfO^{\cdot} + RfO^{\cdot}$	$\longrightarrow$	RfOORf	10^7
13	$Rf^{\cdot} + Rf^{\cdot}$	$\longrightarrow$	RfRf	10^7

[a] $e_m = 1{\cdot}7(\pm 0{\cdot}5) \times 10^{-3}$; $f_2 = 0{\cdot}35 \pm 0{\cdot}06$. For definitions, see text.
[b] M = monomer; Rf$^{\cdot}$, RfO$^{\cdot}$ and $RfO_2^{\cdot}$ represent all types of carbon-centred radicals, alkoxy radicals and peroxy radicals, respectively.

From the mechanism shown in Table 1, a system of differential equations was derived for the variables of interest:

$$\begin{aligned}
D(O_2) &= -F3 + F8 + F9 - F1 \\
D(M) &= -F1 - F4 - F5 \\
D(-OO-) &= F4 + F9 + F10 + F12 - F2 \\
D(-O-) &= F5 + F11 \\
D(RO) &= F1 + F6 + F7 \\
D(Rf^{\cdot}) &= 2F1 + F4 + F5 + F6 + F7 - F3 \\
&\quad - F10 - F11 - 2F13 \\
D(R_fO_2^{\cdot}) &= F3 - F4 - 2F8 - 2F9 - F10 \\
D(R_fO^{\cdot}) &= 2F2 + 2F8 - F5 - F6 - F7 - F11 \\
&\quad - 2F12
\end{aligned}$$

where Fn are the reaction terms and RO, (—OO—) and (—O—) represent the concentrations of carbonyl products, peroxides and ether bonds, respectively. The rate terms for the initiation [reaction(1)] and the photoscission of peroxides [reaction (2)] are described by the equations

$$F1 = e_m[M]\Sigma I_j[1 - \exp(-S_jL)]/S_j \quad (1)$$

$$F2 = f_2\Sigma e_j[X]\, I_j[1 - \exp(-S_jL)]/S_j \quad (2)$$

$$S_j = e_m[M] + e_j[ROOR] \quad (3)$$

where I_j are the initial intensities at the different wavelengths in the UV spectrum; e_j are the molar absorption coefficients for peroxides at the different wavelengths of the lamp spectrum: these coefficients were determined in separate experiments by using samples of peroxidic polyethers purposely prepared by photo-oxidation of HFP; the use of these coefficients in equation (2) allows the model to account for the rate of radical production from the major source (peroxides) and also for the effects eventually arising from the changes of the UV spectrum across the sample due to the wavelength dependence of the absorptivity of peroxides; e_m = molar absorption coefficient for the monomer; f_2 = efficiency factor for radical production in the photoscissions of the peroxides; and L = optical path length. The system of kinetic differential equations was integrated numerically without a steady-state approximation by adopting the modified Gear stiff method based on a backward difference algorithm with automatic control of step size and order.[11]

The decisive advantage of this method over other 'historical' routines (Runge–Kutta, Adams–Moulton, etc.) relies on the fact that it allows mechanisms with very large differences in the reaction parameters to be handled without requiring unacceptable computing times (the stiffness problem); it is thus possible to perform high-precision calculations of the time dependence of the concentration variables in complex mechanisms without recourse to the algebraic reduction of the system of differential equations by the steady-state and rate-determining step approximations.[11b] The Gear routine was inserted into a best-fit program which was based on the Levemberg–Marquant algorithm, which combines the gradient and Newton methods with the jacobian calculated by forward difference approximations. At each call the Gear routine allows the updating of the error function $F = \Sigma[(C_{ci} - C_{si})^2]^{1/2}$, where C_{ci} and C_{si} are the weighted calculated and experimental observations, respectively.

The rate constants for reactions (4)–(7), the efficiency factor f_2 and the molar absorption coefficient e_m pertaining to the reaction (1) were used as fitting parameters. The rate constants for mutual couplings of peroxy radicals [reactions (8) and (9)] were also treated as fitting parameters; however the validity of the best-fit predictions for these latter constants could be checked satisfactorily by comparison with the experimental values determined under similar conditions[12] (see below). The variations of the parameters were scaled in order to produce comparable effects on the objective function. Convergence of the best-fit procedure was assumed to be achieved when the variations of the error function in two successive iterations was less than 10^{-4}. The reference experimental data used for the identification of the model were the time dependences of the oxygen uptake, the consumption of the monomer, the build-up of peroxides, the build-up of the ether groups and also the total yield of carbonyls and the weight-average molecular weight, both measured at the end of the reactions. Separate best-fit calculations were performed for each of the eight sets of experimental data obtained under different experimental conditions and the eight sets of best-fit parameters thus derived were used to obtain the average values and the average errors reported in Table 1. Attempts to match the experimental observations by reducing the number of the fitting parameters one at a time conclusively showed that all the parameters are necessary and sensitive.

RESULTS AND DISCUSSION

Reaction mechanism

The results of the kinetic simulations are summarized in Tables 2 and 3. For conciseness, in Table 3 only the data pertaining the end reaction times are reported but the best fits were based also on observations at the intermediate times as in Table 2 (available on request). The model is capable of reproducing the six experimental variables over the entire range of reaction times and correctly predicts the effect of the light intensity and reactor volume on the overall reaction rates and kinetic chain lengths. It is therefore inferred that the model is suitable for representing the main features of the photo-oxidation process. According to the reaction scheme and the best-fit rate constants reported in Table 1, the dominant source of peroxides is predicted to be the propagation based on the addition of peroxy radicals to the monomer (70 per cent). However, the

Table 2. Kinetic simulation of the photo-oxidation of hexafluoropropene: experimental and computed concentrations obtained with an optical path length $L = 1$ cm and variable light intensity (I)

		Monomer (mol l^{-1})		O_2 (mol l^{-1})		—OO— (mol l^{-1})		—O— (mol l^{-1})		RR'C=O (mol l^{-1})	M_w/166,
Conditions	t(min)	Exp.	Calc.	Exp.	Calc.	Exp.	Calc.	Exp.	Calc.	Calc.[a]	Calc.
$L = 1$ cm, $I = 0{\cdot}76 \times 10^{-5}$ E s^{-1}											
	50	10·45	10·47	0·03	0·12	0·035	0·034	—	0·153	0·01	42·1
	75	10·25	10·30	0·16	0·22	0·054	0·057	—	0·30	0·019	39·8
	100	10·00	10·01	0·29	0·34	0·080	0·083	—	0·486	0·032	39·1
	125	9·75	9·83	0·47	0·49	0·095	0·110	—	0·710	0·046	38·0
	150	9·45	9·53	0·65	0·65	0·130	0·139	—	0·960	0·064	37·1
	175	9·15	9·24	0·85	0·83	0·160	0·167	—	0·123	0·083	36·3
	200	8·80	8·92	1·06	1·02	0·190	0·196	—	0·153	0·103	35·6
	225	8·50	8·59	1·25	1·21	0·220	0·224	—	0·183	0·126	35·0
	250	8·15	8·25	1·45	1·40	0·255	0·252	—	2·140	0·150	34·4
	275	7·80	7·90	1·64	1·61	0·280	0·278	2·66	2·410	0·176	33·8
	300	7·45	7·55	1·83	1·81	0·310	0·304	2·93	2·790	0·203	33·3
	325	7·15	7·20	2·02	2·00	0·335	0·330	3·21	3·110	0·238	32·8
	350	6·85	6·85	2·21	2·21	0·350	0·350	3·48	3·430	0·261	32·3
	375	6·55	6·51	2·36	2·40	0·375	0·374	3·75	3·760	0·290	31·8
	400	6·25	6·17	2·52	2·60	0·395	0·395	4·03	4·070	0·325	31·3
	425[a]	6·00	5·84	2·67	2·80	0·410	0·415	4·30	4·390	0·358	30·9
$L = 1$ cm, $I = 0{\cdot}29 \times 10^{-4}$ E s^{-1}											
	50	8·95	9·30	0·85	0·74	0·085	0·074	1·54	1·22	0·082	33·4
	100	6·57	7·56	2·25	1·73	0·155	0·145	2·93	2·92	0·209	28·5
	150	5·05	5·84	3·15	2·70	0·205	0·202	4·32	4·57	0·360	25·0
	175	4·70	5·07	3·39	3·13	0·215	0·224	5·00	5·31	0·445	23·5
	200	4·20	4·38	3·63	3·53	0·225	0·245	5·71	5·98	0·532	22·2
	225	3·85	3·76	3·82	3·89	0·250	0·257	6·40	6·58	0·622	20·9
	250[b]	3·50	3·22	4·02	4·22	0·255	0·269	7·10	7·11	0·710	19·7

[a] Exp. RR'C=O at 425 min = 0·35 mol l^{-1}. Exp. M_w/166 at 425 min = 31·0.
[b] Exp. RR'C=O at 250 min = 0·65 mol l^{-1}. Exp. M_w/166 at 250 min = 22·0.

contribution to terminal couplings of peroxy and alkoxy radicals is significant (25 per cent and 5 per cent, respectively). A propagation cycle based on the non-terminal disproportionation of peroxy radicals to alkoxy radicals followed by the addition of alkoxy radicals to the monomer is predicted to be the major pathway for the consumption of the monomer, being substantially faster than monomer addition to peroxy radicals. The stationary concentration of intermediate radicals is calculated to decrease in the order $[R_fO_2^{\cdot}]\,10^{-5}$M > $[R_fO^{\cdot}]\,10^{-6}$M > $[R_f^{\cdot}]\,5 \times 10^{-9}$M (Figure 2). As a consequence, the major terminative

Table 3. Kinetic simulation of the hexafluoropropene photo-oxidation: experimental and calculated results for runs performed with variable optical path length (L) and light intensity (I)[a]

			Monomer (mol l^{-1})		O_2 (mol l^{-1})		—OO— (mol l^{-1})		—O— (mol l^{-1})		RR'C=O (mol l^{-1})		M_w/166	
t (min)	L (cm)	I[b]	Exp.	Calc.	Exp.	Calc.	Exp.	Calc.	Exp.	Calc.	Exp.	Calc.	Exp.	Calc.
250	2	I_a	4·70	4·59	3·70	3·51	0·27	0·27	5·53	5·81	0·58	0·62	25·0	21·8
325	2	I_b	7·55	7·55	2·11	2·29	0·34	0·33	2·89	2·75	0·18	0·17	35·0	31·0
250	4	I_a	6·05	6·27	2·71	2·55	0·28	0·29	4·15	4·21	0·27	0·28	27·6	28·3
400	4	I_b	8·85	8·59	1·40	1·32	0·29	0·30	2·09	1·89	0·11	0·12	40·0	41·6

[a] For conciseness only the data pertaining to the end reaction times are quoted.
[b] $I_a = 0{\cdot}29 \times 10^{-4}$ E s^{-1}; $I_b = 0{\cdot}76 \times 10^{-5}$ E s^{-1}.

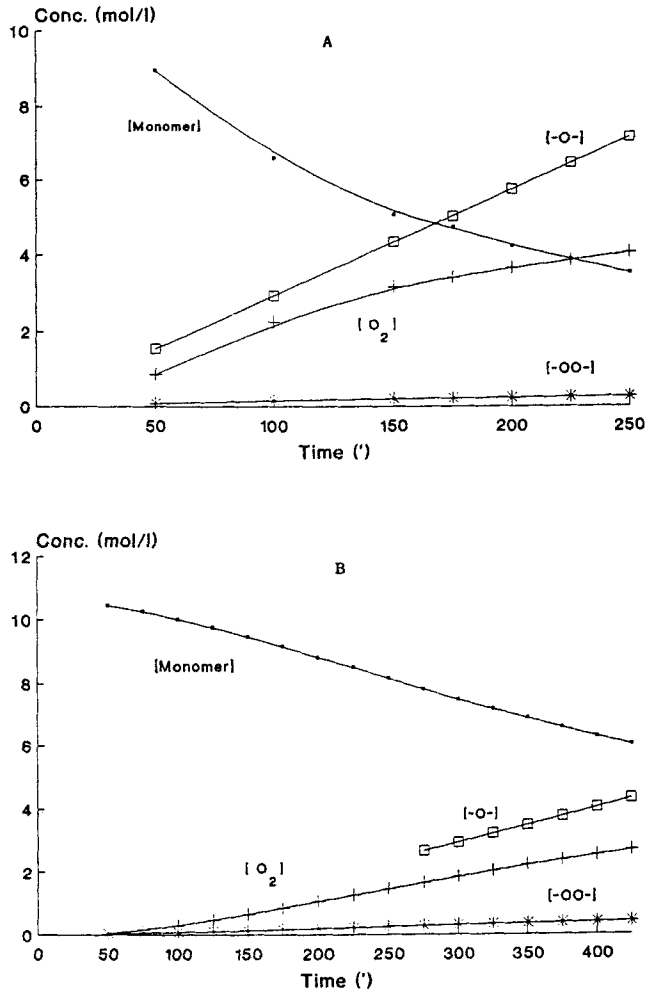

Figure 1. Photo-oxidation of hexafluoropropene. Experimental curves for the oxygen uptake, the monomer consumption and the build-up of peroxidic and ether units. Optical path length $L = 1$ cm. (A) Light intensity $I = 0{\cdot}29 \times 10^{-4}$ E s^{-1}. (B) Light intensity $I = 0{\cdot}76 \times 10^{-5}$ E s^{-1}

mechanism is the coupling of $R_fO_2^{\cdot}$ radicals, which is about five times faster than the coupling of alkoxy radicals. Of negligible importance under the conditions of oxygen partial pressure adopted in the simulation are terminations involving carbon-centred radicals. The model is very sensitive to the rate constants K_4, K_8, K_9, and to the ratios K_5/K_6 and K_5/K_7. These parameters are therefore significant as probes of reactivity in the corresponding classes of reaction.

Addition of peroxyl radicals to double bonds

As stated in the Introduction, a major achievement of the kinetic model is the derivation of the rate constants for a class of reactions of perfluorinated peroxy and alkoxy radicals, not previously reported in the literature. The knowledge of these constants makes possible the evaluation of the effect of fluorine substitution on the reactivity of oxygen-centred radicals. In non-fluorinated systems, the addition of peroxy radicals to double bonds is described as a two-stage process.[13]

$$ROO^{\cdot} + \underset{|}{\overset{|}{C}}{=}\underset{|}{\overset{|}{C}} \longrightarrow ROO\underset{|}{\overset{|}{C}}-\underset{|}{\overset{|}{C}}{\cdot} \qquad (4)$$

$$ROOC-\underset{|}{\overset{|}{C}}{\cdot} \longrightarrow RO^{\cdot} + -\overset{\diagup O \diagdown}{C}-C- \qquad (5)$$

Step (5) competes with the addition of oxygen to the alkyl radical and leads to the formation of epoxide with a relative yield with respect to the hydrogen abstraction ranging from 5 to 100 per cent, depending on the alkene

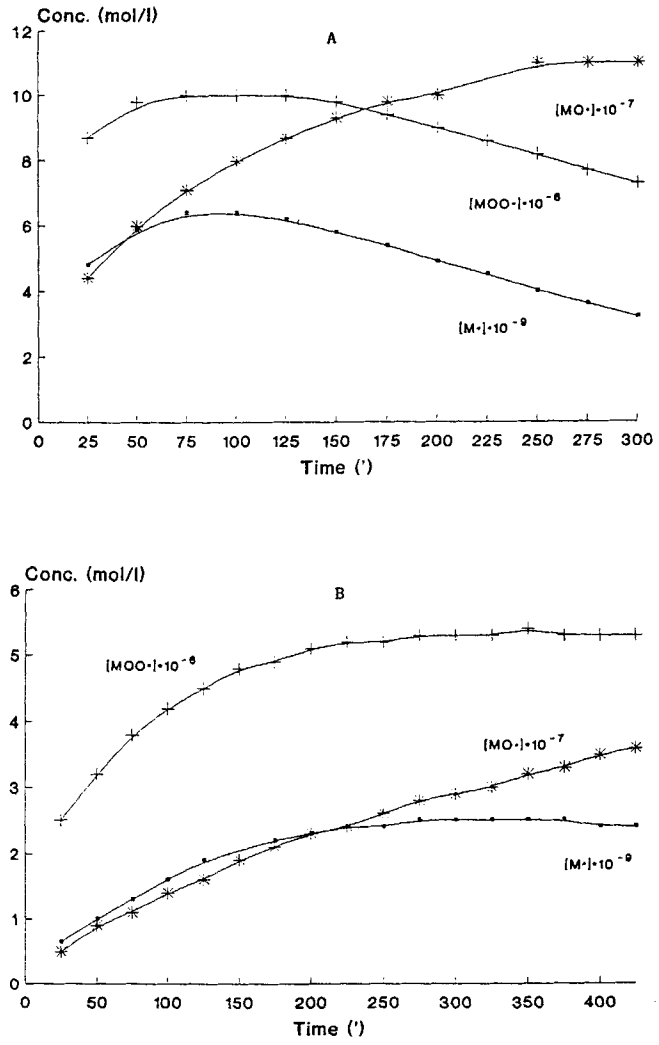

Figure 2. Kinetic model of photo-oxidation of hexafluoropropene. Calculated curves for the build-up and decay of intermediate radicals. Optical path length $L = 1$ cm. (A) Light intensity $I = 0{\cdot}29 \times 10^{-4}$ E s^{-1}. (B) Light intensity $I = 0{\cdot}76 \times 10^{-5}$ E s^{-1}

structure.[14] As a consequence, the overall kinetics are determined by the slower step (4). The rate constants for the addition of isopropyl peroxy radicals to a variety of alkenes were calculated from experimental data reported in the literature[15] and range from *ca* 7×10^{-8} to $0{\cdot}0014$ l mol^{-1} s^{-1} at -40 °C, with $5{\cdot}5 \times 10^{-7}$ l mol^{-1} s^{-1} for propylene. When compared with K_4 (Table 1), these values show that a very large increase of reactivity is induced by perfluorination. The rates of reactions (4) and (5) are reported to increase with decreasing ionization potential of the alkene.[13,15] This observation is consistent with the peroxy radical electrophilicity and transition states of partial ionic character: $ROO^{-}\cdots[CH_2CHCH_3^{+}]$.

The orders of magnitude increase in the reactivity of the perfluorinated system can be explained by the greater polarizability of the perfluoroperoxy radical together with the kinetic vulnerability of the fluoroalkene double bond.[16,17] Another factor is the greater exothermicity of the perfluoroperoxy—carbon bond formation derived from peroxy radical alkene addition[18] [D(RfOO—M) = 284 kJ mol^{-1}].

In propylene, perfluorination induces a lowering of both sigma and orbital levels, causing a significant increase in the ionization potential from 9·7 eV[19] to 11·1 eV.[20] As a consequence, the observed many orders increase in the reaction rate should be attributed entirely to the increase in reactivity of the peroxy

radicals whose electron affinity is expected to be strongly enhanced by perfluorination. Halogenation has recently been shown to increase the rates of electron transfers to peroxy radicals by orders of magnitude.[21] According to PMO theory, reactivity is determined by the SOMO–HOMO interaction (SOMO is of higher energy), which in turn depends on the energy gap. Fluorine substitution at the peroxy radical has a stabilizing effect on the SOMO level, which results in a decrease in the SOMO–HOMO energy gap; this effect is partially counterbalanced by the stabilizing effect of fluorine substituents on the HOMO of hexafluoropropene, which also lowers the orbital energy but to a lesser extent. The net result is a smaller SOMO–HOMO gap and thus a faster reaction in the fluorocarbon vs hydrocarbon system.

With tetrafluoroethylene a different situation applies since only the sigma MO levels of the alkene are lowered by fluorine substitution whereas the HOMO–LUMO levels are substantially unaffected. As a consequence, the vertical ionization potential (*IP*) is nearly identical with that of ethylene [*IP*(ethylene) = 10·6 eV;[22] *IP*(CF_2CF_2) = 10·52 eV[23]]. In this case perfluorination may be predicted to induce a stronger SOMO–HOMO interaction with a consequent greater enhancement of the rate of addition of peroxy radicals to the double bond. The greater reactivity of tetrafluoroethylene over hexafluoropropene in these systems is in accord with the rate constants derived from the kinetic model of tetrafluoroethylene photo-oxidation.[24] Additionally, studies on the co-photo-oxidation of tetrafluoroethylene and hexafluoropropene revealed a relative reactivity ratio of *ca* 300 at −40 °C.[8] The value was partially attributed to the transition-state stabilizing effect arising from partial electron transfer from alkene to peroxy (oxy) radical, a more important process in the C_2 perfluoroalkene for reasons stated above.

The above photo-oxidations afford 30 per cent and negligible yields of fluoroepoxide from tetrafluoroethylene and hexafluoropropene, respectively. While rationalization of this difference may be related to the two-step mechanism proposed for hydrocarbon systems, detailed discussion awaits the collection of further data.

Addition of alkoxy radicals to double bonds

The faster rate of addition of alkoxy radicals to the alkene compared with peroxy radicals is readily rationalized by considering the destabilizing effect on the SOMO arising from lone-pair interactions, which is more pronounced with the peroxy radicals. A comparison with analogue additions in non-fluorinated systems is limited owing to the paucity of kinetic data in the literature. It seems, however, that no dramatic changes in rate constants occur on fluorine substitution of both the alkoxy radical and the alkene, with the previously mentioned exception of tetrafluoroethylene (for the addition of *tert*-butoxy radicals to a variety of olefins, k is estimated to be in the range 30–1000 at −60 °C).[25] This observation supports the notion that a balance exists between stabilization of SOMO and HOMO in the perfluorinated systems.

β-Scission of alkoxy radicals

The kinetics of β-scission are partially determined by the stability of the alkyl radicals produced, which increases with increasing the degree of substitution at the radical centre. As perfluoroalkyl radicals are stabilized by inductive effects, reaction (7) is expected to be faster than scission of *tert*-butoxy radicals [k(*t*-BuO·) = 0·03 s^{-1} at −60 °C[26]]; accordingly, k_6 and k_7 are about 10^4 times greater than k(*t*-BuO·) and are found to be comparable to the rate constants of other non-fluorinated alkoxyls yielding tertiary alkyl radicals.[27]

Further, fluoroalkoxy radical β-scission reactions liberate a neutral molecule, either carbonyl fluoride [reaction (7)] or a substituted acid fluoride [reaction (6)]. Previous work in our laboratories indicates reaction (7) is faster than reaction (6), i.e. at −60 °C β-scission from tetrafluoroethylene oxidation proceeds where that for hexafluoropropylene oxidation slows to the limit of detection. Significant resonance energy has been attributed[16] to the interaction between an electron pair of fluorine and an adjacent carbonyl bond. The fact that transition states from β-scission reactions resemble final products supports the position that reaction (7) is faster than reaction (6), since the former liberates COF_2, which has two fluorine substituents in resonance with a carbonyl group whereas the latter (RfCOF) has only one. The explanation can be extended to the observed rate acceleration of the fluoroalkoxy [reactions (6) and (7)] over alkoxy hydrocarbon radical β-scission reactions by taking into consideration that formaldehyde or acetaldehyde does not have such resonance stabilization.

Terminating couplings of peroxy radicals

The rate constant for terminating couplings of peroxy radicals [reactions (8) and (9)] as derived from the model is in good agreement with that obtained by direct kinetic ESR measurements.[12] This constant is seen to be many orders of magnitude greater than that expected from tertiary non-fluorinated analogues [$2k_t$(*t*-BuOO·) = 7·3 l mol^{-1} s^{-1} at −60 °C[28]]. An explanation of this dramatic fluorine substituent effect has been related to interaction of the HOMO of the polyoxide system with the σ antibonding orbitals of the C—F bonds, which is expected to stabilize the hypothetical tetraoxide intermediate. This stabilization may

result in an acceleration of the irreversible decomposition to alkoxy radicals and dialkyl peroxides and contemporaneously to an increase in the activation energy for the back dissociation to peroxy radicals.

REFERENCES

1. (a) D. Sianesi, A. Pasetti, R. Fontanelli, G. C. Bernardi and G. Caporiccio, *Chim. Ind. (Milan)* **55**, 208 (1973); (b) F. Ciampelli, M. Tacchi Venturi and D. Sianesi, *Org. Magn. Reson.* **1**, 281 (1969)..
2. A. Faucitano, A. Buttafava, G. Caporiccio and C. T. Viola, *J. Am. Chem. Soc.* **106**, 4173 (1984).
3. A. Faucitano, A. Buttafava, F. Martinotti, A. Staccione and G. Marchionni, paper presented at the XIIIth International Conference on Photochemistry, Budapest, 9th August 1987.
4. N. M. Baranova and V. A. Poluetkov, *Khim. Vys. Energ.* **21**, 446 (1987).
5. N. M. Baranova, V. A. Poluetkov and V. G. Verskumov, *Khim. Vys. Energ.* **29**, 1299 (1987).
6. A. Faucitano, A. Buttafava, F. Martinotti and G. Marchionni, in *IUPAC International Symposium on Free Radical Polymerization: Kinetics and Mechanisms, Santa Margherita (Italy), May 1987*, p. 280.
7. D. Sianesi, A. Pasetti and C. Corti, *US Pat.* 3 442 942 (1969).
8. G. Marchionni, U. DePatto and R. J. DePasquale, paper presented at the 12th International Fluorine Symposium, Santa Cruz, California, 1988, abstr. No. 333.
9. E. S. Huyser, *Free-Radical Chain Reactions*, p. 342. Wiley-Interscience, New York (1970).
10. K. R. Ryan and I. C. Plumb, *J. Phys. Chem.*, **86**, 4678 (1982).
11. (a) C. W. Gear, *Comm. Assoc. Comput. Mach.* **14**, 176 (1976). (b) A. Faucitano, H. Atarot, F. Martinotti, V. Comincioli, S. Cesca and S. Arrighetti, *J. Polym. Sci.* **18**, 2175 (1980).
12. A. Faucitano, A. Buttafava, F. Martinotti, G. Marchionni and R. J. DePasquale, *Tetrahedron Lett.* **29**, 5557 (1988).
13. T. V. Filippova and E. A. Blyumberg, *Russ. Chem. Rev.* **51**, 582 (1982).
14. D. E. Van Sickle, F. R. Mayo, R. M. Arluck and M. G. Syz, *J. Am. Chem. Soc.* **89**, 967 (1967).
15. M. I. Sway and D. J. Weddington, *J. Chem. Soc., Perkin Trans. 2* 139 (1983).
16. B. E. Smart, in *Molecular Structure and Kinetics*, edited by J. F. Liebman and A. Greenberg, Vol. 3, p. 141. VCH, Weinheim (1986).
17. E. A. Carter and W. A. Goddard, *J. Am. Chem. Soc.* **110**, 4077 (1988).
18. J. S. Francisco and I. H. Williams, *Int. J. Chem. Kinet.* 455 (1988).
19. R. Bralsford, P. V. Harris and W. C. Price, *Proc. Roy. Soc. London, Ser. A.* **258**, 459 (1960).
20. D. J. Pasto and J. K. Borchardt, *J. Am. Chem. Soc.* **96**, 6220 (1974).
21. Z. B. Alfassi, S. Mosseri and P. Neta, *J. Phys. Chem.* **91**, 3383 (1987).
22. R. E. Homing, *J. Chem. Phys.* **16**, 105 (1948).
23. C. R. Brundle, M. B. Robin, N. A. Kuebler and H. Basch, *J. Am. Chem. Soc.* **94**, 1451 (1972).
24. A. Faucitano, A. Buttafava, G. Marchionni, A. Staccione and R. J. DePasquale, paper presented at the 9th Winter Fluorine Conference, St. Petersburg, Florida, January 1989, abstr. No. 52.
25. J. K. Kochi, *Free Radicals*, Vol. II, p. 694. Wiley, New York (1973).
26. P. Gray, R. Shaw, J. C. J. Thynne and G. Porter, *Progress in Reaction Kinetics*, p. 463. Pergamon Press, Oxford (1967).
27. K. Yul Choo and S. W. Benson, *Int. J. Chem. Kinet.* 833 (1981).
28. J. A. Howard, *Isr. J. Chem.* **24**, 33 (1984).